

Design and Implementation of PV Integrated UPQC with ANFIS Controller

Dr.BUCIO PITYY

PG Student , Dept of EEE, S V University college of Engineering, Tirupati.

Dr.RAMACHANDRA C G

Assistant Professor, Dept of EEE, S V University college of Engineering, Tirupati.

:

The ANFIS controller and the PV integrated UPQC system are evaluated in this research. The primary objective is to use an ANFIS controller to manage the dc-link voltage. During sags and swells, the compensator injects voltage that is either in phase or out of phase with the voltage at the common connection (PCC). For improved performance, the load active current component of the photovoltaic-based unified power quality controller (PV UPQC) system is evaluated using a moving average filter-based reference. Clean energy generation, improved power quality, and lower harmonic distortion are just a few of the system's advantages. Under sag and swell conditions, the compensator injects voltage that is in phase or out of phase with the PCC voltage. Among other things, the MATLAB/SIMULINK software is used to model load unbalancing, PCC voltage sags/swells, and irradiation fluctuations.

KEYWORDS:

ANFIS (adaptive neuro-fuzzy inference system) controller, PV (photovoltaic) , MPPT (maximum power point tracking), shunt compensator, series compensator, UPQC (unified power quality controller), shunt compensator and series compensator.

I.

In terms of grid power quality, distributed generation (DG) systems have both advantages and downsides (PQ). They can improve system efficiency by generating power locally. Customers can have more stable and uninterrupted power while saving money on energy [1]. The use of distributed generation in the grid is increasing around the world. Denmark, for example, has a significant penetration of wind energy, with 14 percent of the country's total electrical energy consumption coming from wind [2]. According to an EPRI analysis, by 2010, DG will account for 25% of new generation and at least 20% of the total electrical utility market, worth USD 72 billion [3].

In the near future, deregulation of the electricity market may lead to a higher level of DG penetration from renewable energy sources (wind, solar, biomass, etc.) [4]. In terms of environmental protection, DG derived from renewable energy sources is critical, as it reduces harmful emissions. Because most DG systems connect to the grid via a power electronic interface, the introduction of higher frequency harmonics into the system is unavoidable. As a result, if not addressed effectively, other grid integration issues are similarly concerning in terms of electrical pollution. Variable wind speed, solar and tidal power variations, and so on are uncontrollable variables that will inevitably alter the quality of the generated power.

Active filtering techniques for incorporation into integrating power electronic converters are being investigated [2,5], however they must be case specific. Because PQ varies depending on the kind of generation source, a common PQ platform for sensitive non-linear loads in the distribution system is necessary. As a result, suitable power conditioning interfaces are recommended for sensitive non-linear loads. The most prevalent categories of loads include production sectors (such as automobile factories, paper mills, chemical and pharmaceutical industries, semiconductor manufacturing facilities, and so on) and critical service providers (such as medical centres, airports, and broadcasting centres). Common grid integration challenges include voltage and frequency compatibility, as well as the requirement for active and reactive power.

Two UPQC models are reviewed and analysed in this work from the perspective of VA loading and applications. UPQC is a functionally combined series and shunt active filter that maintains the required quality of both the input voltage and current.

A power conditioning device can act as an interface between the grid and sensitive loads, allowing the load to be unaffected by variations in utility power quality. The unified power quality conditioner (UPQC) [6, 7] is the most comprehensive power conditioning device that can eliminate both voltage and current quality issues.

- In the proposed controller evaluate the accurate value compare to the PI controller.
- The proposed controller less harmonics compare to the existing controller.
- The steady state error reduced in the ANFIS based controller.

In both dynamic and steady-state scenarios, the performance of the proposed system is thoroughly examined using Matlab-Simulink software.

II.

A three-phase UPQC system is required for the PV-UPQC. The PVUPQC is made up of a shunt and a series compensator that are both connected to the same DC bus. The load side is where the shunt compensator is attached. Through a reverse blocking diode, the solar PV array is directly connected to UPQC's DC-link. The series compensator compensates for grid voltage sags/swells while in voltage control mode. Interface inductors connect the grid to the shunt and series compensators. The voltage generated by the series compensator is injected into the grid via a series injection transformer. Ripple filters are used to filter harmonics caused by converter switching activity. To make a nonlinear load, a bridge rectifier and a voltage-fed load are used. The schematic diagram of the PV-UPQC system depicted in figure.1.

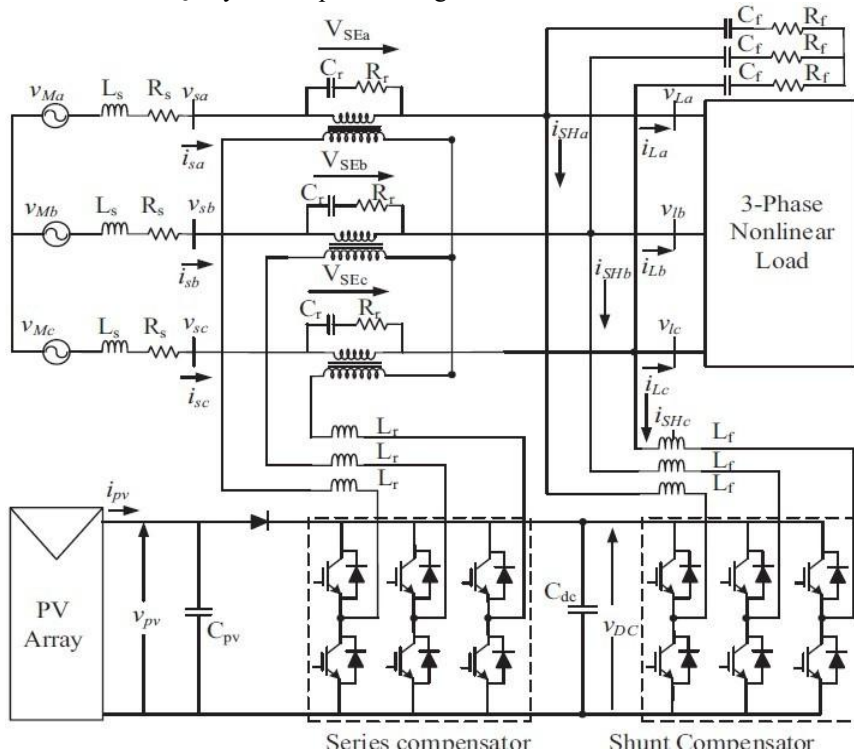


Figure 1. PV – UPQC System Configuration

PV-UPQC design starts with suitable PV array dimensions, DC-link capacitor sizing, DC-link voltage levels, and so on. In addition to compensating for load current reactive power and current harmonics, the shunt compensator is sized to regulate the peak power output from the PV array. Because it is directly connected to UPQC's DC-link, the PV array is sized so that the MPP voltage is the same as the intended DC-link voltage. Under normal conditions, the rating assures that the PV array provides active electricity to the load while also feeding power into the grid. The interfacing inductors for the series and shunt compensators, as well as the series injection transformer for the series compensator, have all been developed. The following is a summary of the UPQCs for PV design.

a)

The value of the dc-link voltage can be analyzed by using eq (1)

$$dc = 2 \frac{\sqrt{2}V_{LL}}{\sqrt{3}m} \quad (1)$$

Where

$$m = \frac{V_{LL}}{V_{dc}} = \frac{415}{700} = 0.593$$

b)

The ripple current, switching frequency, and DC-link voltage all affect the interfacing inductor rating of a shunt compensator. The interfacing inductor is written like this:

$$L_{sh} = \frac{\sqrt{3} V_{dc} * m}{12 * f_{sh} * I_{cr,pp}} \quad (2)$$

Where

m is the modulation depth,

a is the maximum overload pu value,

f_{sh} is the switching frequency,

$I_{cr,pp}$ is the inductor ripple current.

c)

The PV-UPQC is designed to support a 0.3 Pu sag/swell (71.88 V). The injection voltage is just 71.88 V when the DC-link voltage is 700V, resulting in a low modulation index for the series compensator. The modulation index of the series compensator should be kept near to unity to run the series compensator with the fewest harmonics. As a result, a series transformer with a high turn ratio is used.

$$K_{SE} = \frac{V_{VSC}}{V_{SE}} \quad (3)$$

The value of K_{SE} was discovered to be 3.33. The chosen number is three. The following is the rating of the series injection transformer:

$$S_{SE} = 3 * S_{SE,sag} \quad (4)$$

$$I_r = \frac{\sqrt{3} * m * V_{dc} * K_{SE}}{12 * S_{SE,r}} \quad (5)$$

The modulation depth is denoted by m , the maximum overload Pu value is denoted by a , the switching frequency is denoted by f_{se} , and the inductor current ripple is denoted by I_r .

III. PV – UPQC Control

A.

The shunt compensator extracts the greatest electricity from the solar PV array by operating it at maximum power. The maximum power point tracking (MPPT) approach is used to produce the reference voltage for PV-DC-link UPQCs. Two prominent MPPT algorithms are Perturb and Observe (P& O) and incremental conductance (INC). In this work, the (P& O) technique is used to implement MPPT. To keep the DC-link voltage at the created reference, a PI-controller is employed. The shunt compensator corrects for load current by using the active fundamental component of the load current.

The load currents are converted to the d-q-0 domain using the phase and frequency information provided from the PLL. The PLL input is the PCC voltage. The d-component of the load current (I_{ld}) is filtered in the abc frame of reference to produce the DC component (I_{ldf}), which represents the basic component. To recover the DC component without compromising dynamic performance, a moving average filter (MAF) is used. A moving average filter's transfer function is,

$$G(s) = \frac{1 - e^{-T_{ws}}}{ws} \quad (6)$$

The window length of the moving average filter is T_{ws} . Because the lowest harmonic present in the d-axis current is a double harmonic component, T_{ws} is kept at half of the fundamental time period.

The MAF has a DC gain of one and a gain of zero for integer multiples of the window length.

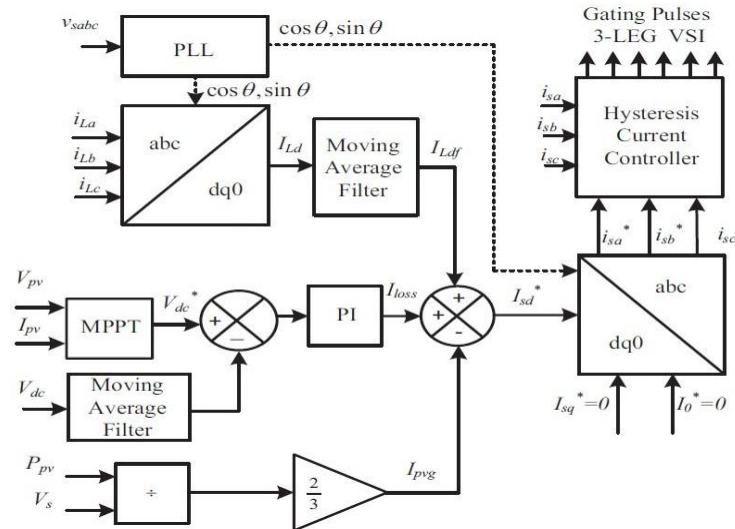
The PV array's current component is denoted by I_{pv} .

$$I_{pv} = \frac{P_{pv}}{V_s} \quad (7)$$

V_s is the magnitude of the PCC voltage, and P_{pv} is the PV array power. In the d-axis, the current state of the reference grid is written as.

$$I_{sd}^* = I_{Ldf} + I_{loss} - I_{pvg} \tag{8}$$

I_{sd}^* Currents in the abc domain are converted to grid currents in the abc domain. The reference grid currents are compared to the measured grid currents in a hysteresis current controller to generate the gating pulses for the shunt converter.



B.

Before compensation, in-phase compensation, and energy optimal compensation are the three series compensator control techniques. The several compensation mechanisms utilised for series compensator control are thoroughly explained. The series compensator is used in this study to inject voltage in the same phase as the grid voltage, resulting in the least amount of voltage injection possible. The series compensator's control structure is depicted in Figure 3. The basic component of PCC voltage is extracted using a PLL, and the dq-0 domain reference axis is built. The reference load voltage is built using the phase and frequency information from the PLL-collected PCC voltage. The PCC and load voltages are converted using the d-q-0 domain.

Because the reference load voltage must be in phase with the PCC voltage, the d-axis component value of load reference voltage is the peak load reference voltage. The q-axis component is maintained at zero. The difference between the load reference load voltage and the PCC voltage determines the actual series compensator voltages. The difference voltage and the PCC voltage determine the series compensator's reference voltage. To create appropriate reference signals, PI controllers exploit the difference between reference and actual series compensator voltages. These signals are translated to the abc domain and delivered via a pulse width modulation (PWM) voltage controller to provide enough gating signals for the series compensator.

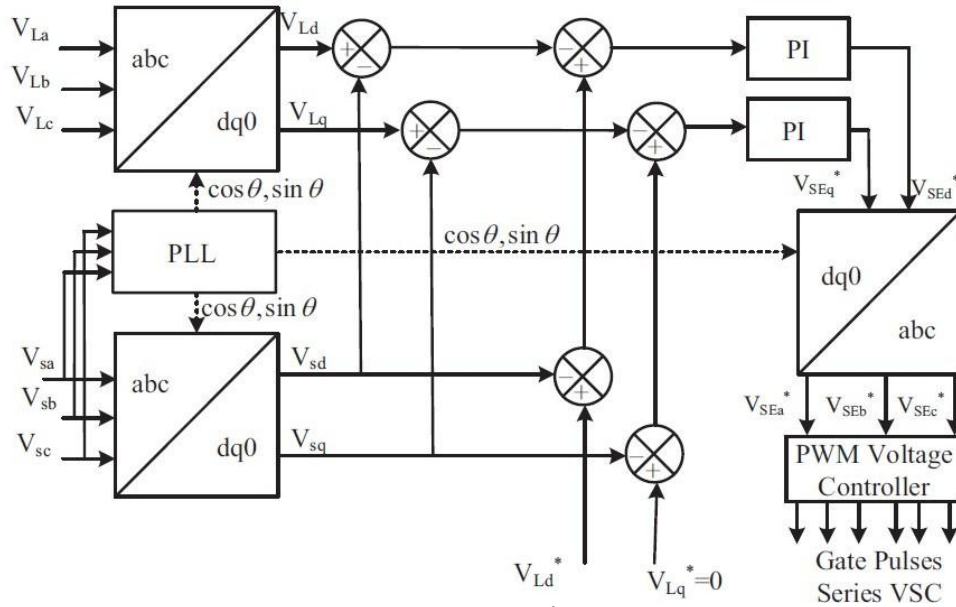


Figure 3. Series Compensator's control structure.
IV.

The adaptive Neuro fuzzy Inference system (ANFIS) is a data-driven approach for resolving trademark guessing issues using a neural organisation strategy. Information-driven ANFIS network union solutions are frequently based entirely on grouping a prepared set of mathematical examples of the cryptic trademark to be approximated. ANFIS networks have been successfully applied to class liabilities, rule-principally based technique control, design notoriety, and comparative concerns since their introduction. The fuzzy adaptation provided by Takagi, Sugeno, and Kang to codify a logical technique to deal with creating fuzzy parameters from an information output records set is included in this fuzzy logic controller.

a)

For the sake of simplicity, the fuzzy inference system under discussion is supposed to have two inputs and one output. The fuzzy if-then rules of Takagi and Sugeno's type are found in the rule base as follows:

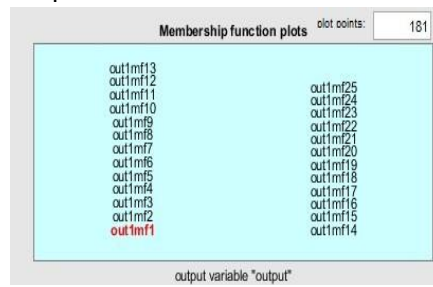
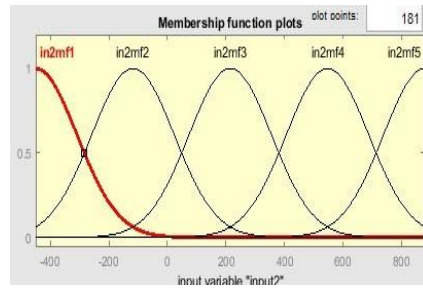
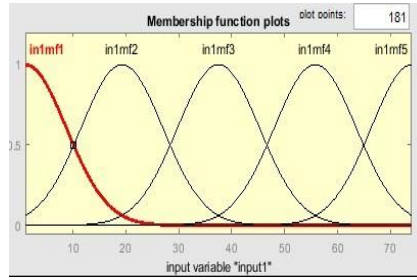
$$\text{Assuming } x \text{ is } A \text{ and } y \text{ is } B \text{ then } z \text{ is } f(x, y)$$

Where A and B are the antecedents' fuzzy units, and $z = f(x, y)$ is a new trademark in the following. For the enter factors x and y, $f(x, y)$ is a polynomial.

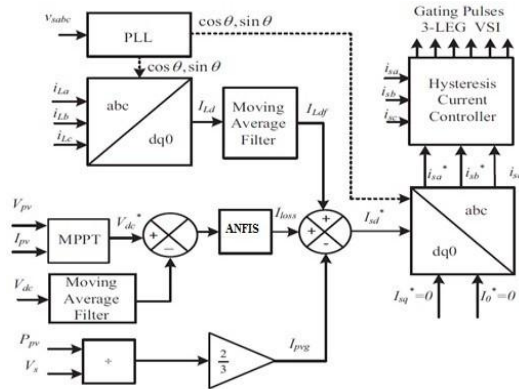
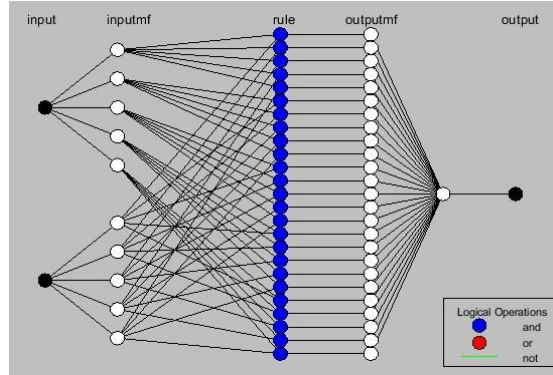
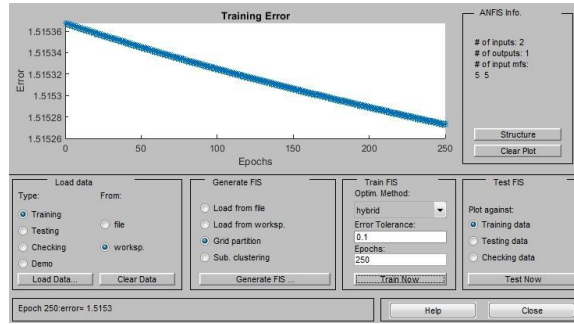
The ANFIS regulator has input membership functions, and one of these functions is participation. Figures 4 to 6 depict schematic charts of information and result membership functions. The number of cycles used and the parameters shown in table 1 were used to reduce the error. Mamdani-based fuzzy logic controllers and Sugeno-based fuzzy logic controllers are the two types of fuzzy logic controllers. The regulator has tutoring FIS (fish kind deduction framework) kind and emphases in the ANFIS based absolutely regulator type as Sugeno.

" ,NS for
,EZ for ,PS for ,"

" . " The input membership functions are all five, and the change in error is also five. There are a total of 25 emphases in the overall regulations. The cycles can be used with the use of entrance and yield tactics. The ANFIS regulator is used to demonstrate the design of ANFIS in Figure 8 and the preparation botches in Figure 7.



E/C E	NB	NS	EZ	PS	PB
NB	OUTMF1	OUTMF2	OUTMF3	OUTMF4	OUTMF5
NS	OUTMF6	OUTMF7	OUTMF8	OUTMF9	OUTMF10
Z	OUTMF11	OUTMF12	OUTMF13	OUTMF14	OUTMF15
PS	OUTMF16	OUTMF17	OUTMF18	OUTMF19	OUTMF20
PB	OUTMF21	OUTMF22	OUTMF23	OUTMF24	OUTMF25



The shunt compensator extracts the greatest power from the solar PV array by operating it at its maximum power point. The maximum power point tracking (MPPT) approach is used to create the reference voltage for PV-DC-link UPQCs. Two common MPPT algorithms are the Perturb and Observe (P& O) algorithm and the incremental conductance algorithm (INC). In this study, the (P& O) method is used to implement MPPT. The DC-link voltage is maintained at the generated reference by an ANFIS-controller. The ANFIS controller is based on the Sugeno technology and has greater performance than the PI controller. Figure 9 shows the schematic diagram of the ANFIS-based controller.

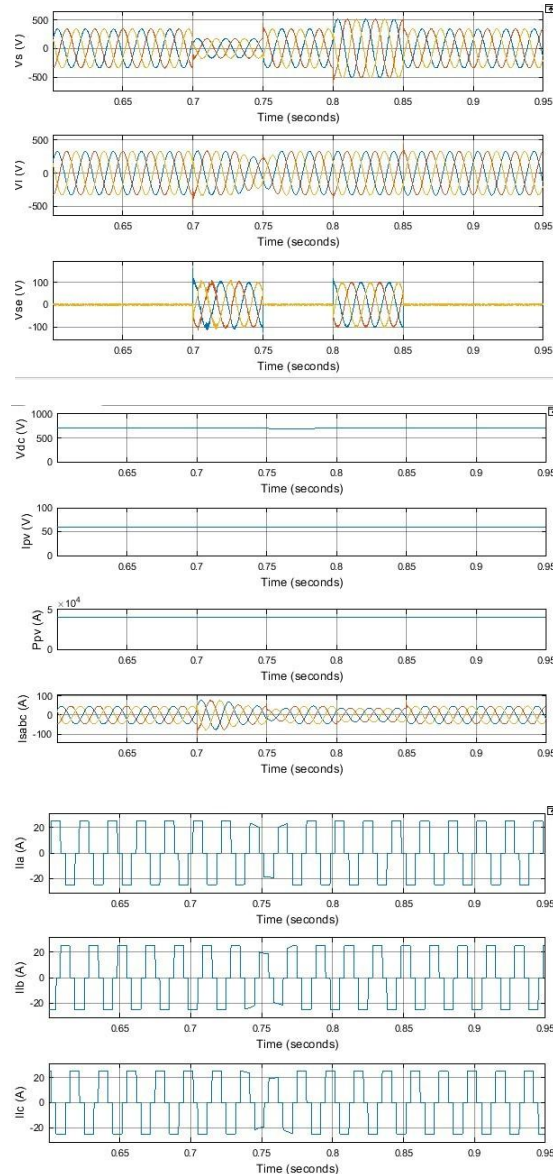
V.

The steady state and dynamic performances of PV-UPQC are examined by simulating the system in Matlab-Simulink software. The load is a nonlinear R-L load consisting of a three-phase diode bridge rectifier. The system is subjected to a variety of dynamic situations, including PCC voltage sag and swell, and PV irradiation change. In Supplement, you'll find the actual framework bounds. Figure 9 depicts the proposed approach schematic graph. The ANFIS regulator and the PI regulator were displayed to evaluate the results of Matlab/Simulink programming. When compared to the PI regulator, the proposed ANFIS controller performs better. In contrast to the suggested regulator work on the general exhibition, which creates harmonics in load current of 23.46 % and grid contemporary of 1.86 %, the PI regulator-based framework produces harmonics in load current of 10.69 % and grid contemporary of 0.27 %. Table 2 shows the THD esteems of the PI and ANFIS regulators as a result of their interactions.

a)

1. PV-UPQC Performance at PCC Voltage Fluctuations

Figure 10 depicts the dynamic universal overall performance of the PV-UPQC with PI controller in the presence of PCC voltage sags/swells. The intensity of the irradiation is maintained at 1000W/m^2 (G). The numerous sensed signals include grid currents (I_s), load currents (I_{la} , I_{lb} , I_{lc}), shunt compensator currents (I_{sha} , I_{shb} , I_{shc}), and solar PV array power (P_{pv}). There is a voltage sag of 0.3pu and a voltage swell of zero between 0.07 and 0.75 seconds. 3pu exists between 0.8 and 0.85 seconds. The collection compensator compensates for grid voltage by injecting a suitable voltage V_{se} in the opposite location of the grid voltage disturbance, allowing the rated load voltage to be maintained.



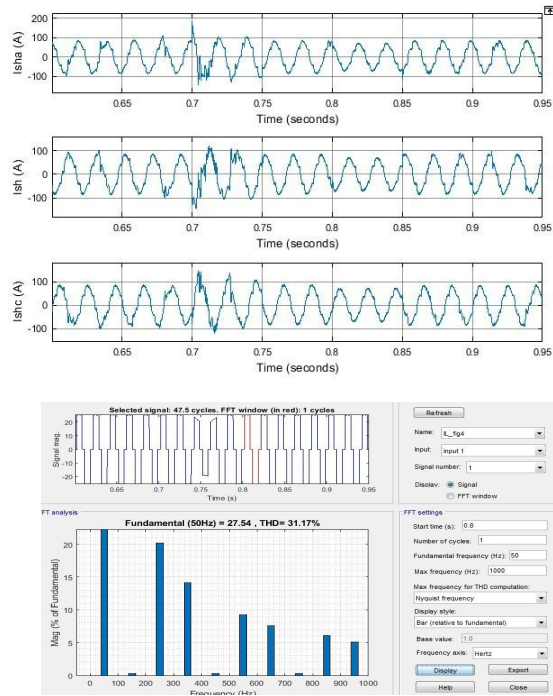
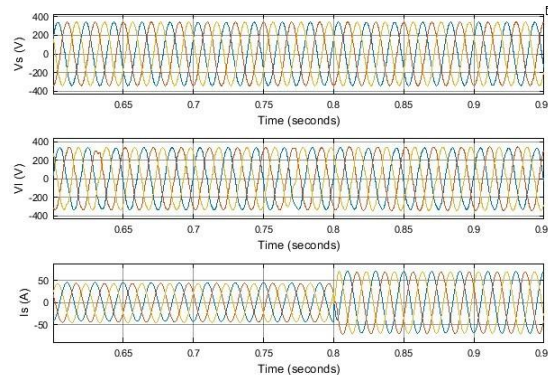


Figure 10. Performance of PV – UPQC under voltage sag and swell conditions.

2. PV-UPQC Performance in Unbalanced Load Conditions

In a load imbalance scenario, Figure 11 shows the dynamic performance of the PV-UPQC with PI controller. At $t=0.8s$, the loads 'b' phase is disconnected. The grid is now sinusoidal and in tune with the electrical element, as can be observed. As a result of the reduction in fundamental strong demand, the current fed into the grid has grown considerably. The DC-link voltage is also constant, and it is maintained near 700 V, which is the required regulated rate.



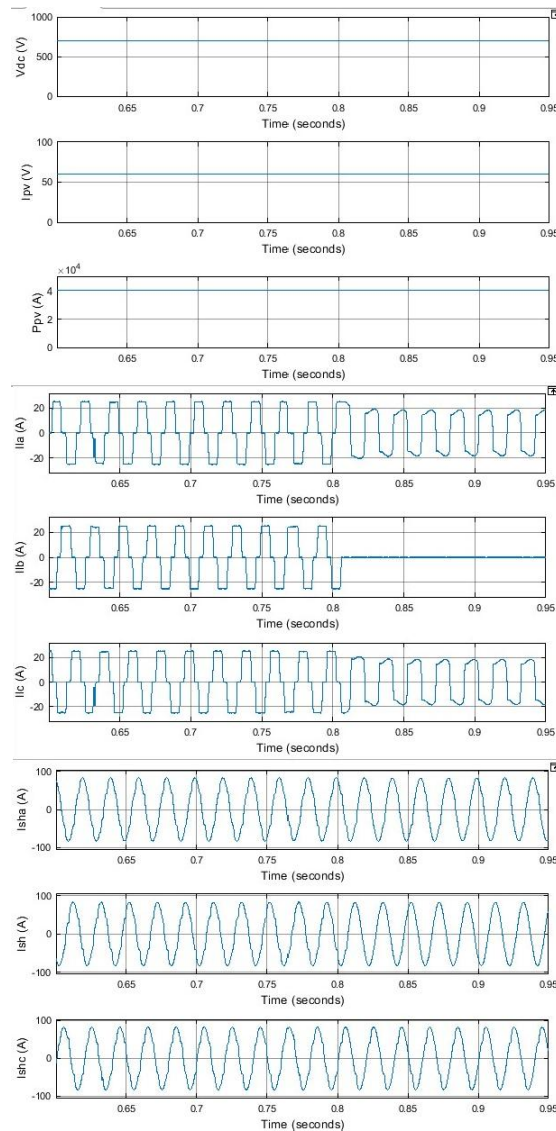
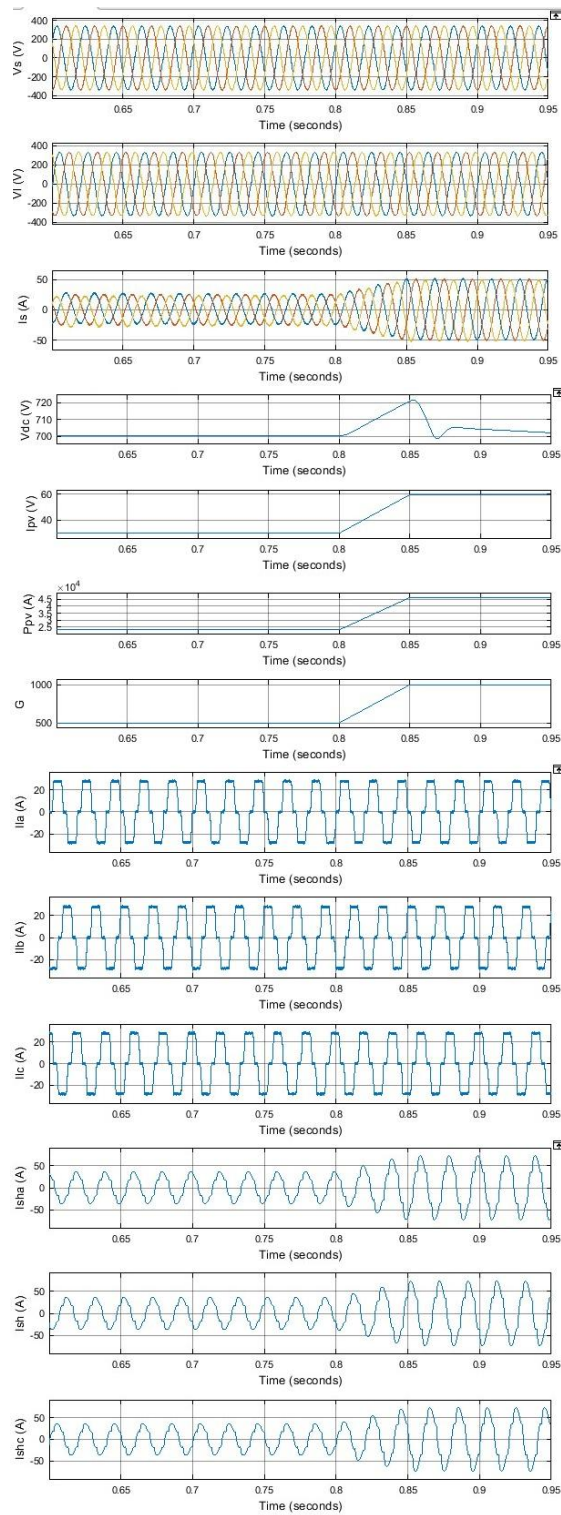


Figure. 11 PV – UPQC performance during a load unbalance condition

3. PV-UPQC Performance Under Various Irradiation

Figure 12 depicts the PV-UPQC with a PI controller's dynamic overall performance as solar irradiation changes. The sun gives off $500\text{W}/\text{m}^2$ at 0.8s and $1000\text{W}/\text{m}^2$ at 0.85s of irradiation. As the PV array's production rises in response to rising irradiation, grid current rises as the PV array feeds electricity into the grid. When it comes to accounting for harmonics caused by load current, the shunt compensator trails behind MPPT. Harmonic spectra and THD load using a PI-based controller for current day-to-day and grid contemporaneous are shown in Figures 13 and 14.



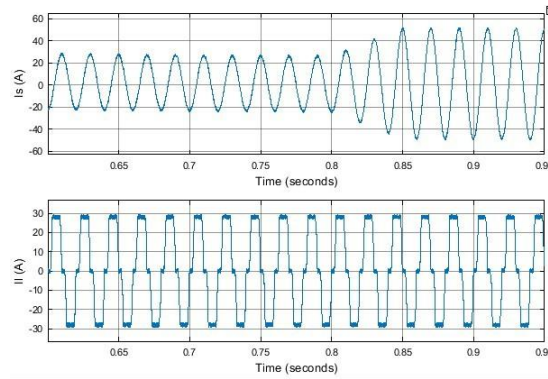
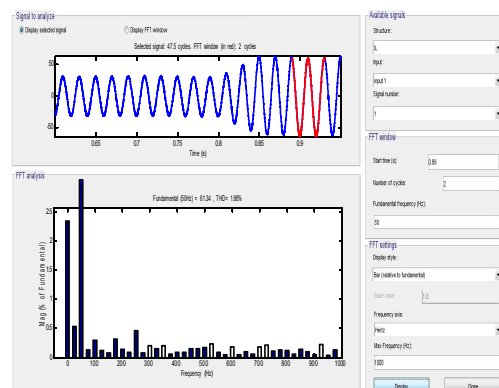
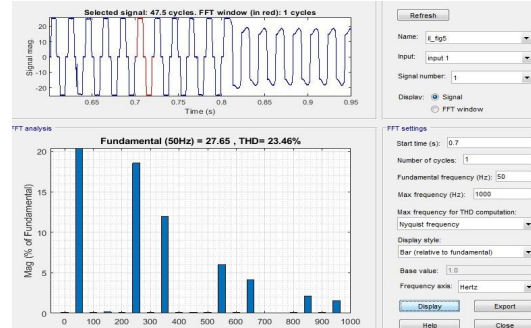


Figure. 12 PV – UPQC Performance under Varying Irradiation Conditions with PI controller



b)

1. PV-performance UPQC's when the PCC voltage fluctuates

In the presence of PCC voltage sags/swells, the dynamic performance of PV-UPQC with ANFIS controller is shown in Fig.15. When the power density is 1000W/m², irradiation (G) is conserved. Only a few of the numerous sensed indications include PCC voltages (V_s), load voltages (V_l), series compensator voltages (V_{SE}), DC-link voltage (V_{dc}), solar PV array current (I_{pv}), solar PV array energy (P_{pv}), grid currents (I_s), load currents (I_{la}, I_{lb}, I_{lc}), and shunt compensator currents (I_{sha}, I_{shb}, I_{shc}). The collection compensator compensates for grid voltage disturbances in some cases by injecting an appropriate voltage V_{se} into the opposite segment, allowing the load voltage to remain at rated value. There could be a voltage sag of zero.3pu and a voltage swell of 0.3pu between 0.7 and 0.75s, and a voltage swell of 0.3pu between zero.8 and 0.85s.

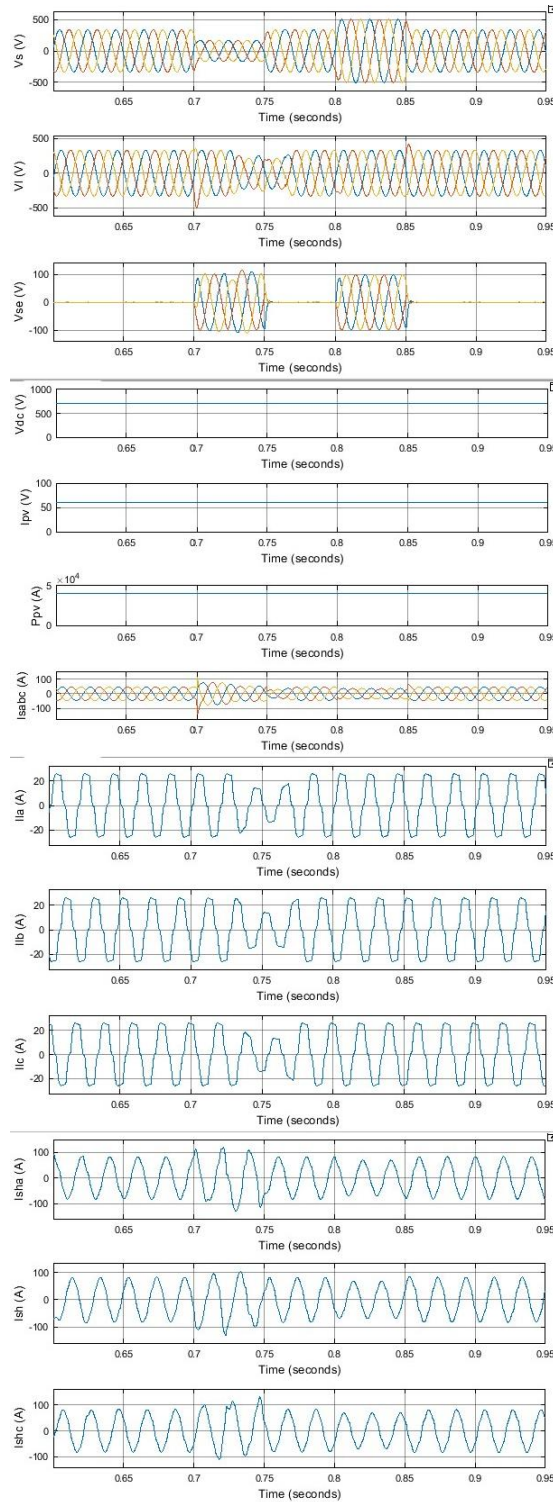


Figure 15: PV – UPQC performance with ANFIS controller during voltage sag and swell conditions.

2. PV-UPQC Performance under Unbalanced Load Conditions

Figure 16 shows the PV-UPQC with ANFIS controller's dynamic fundamental performance when the load is unbalanced. The 'b' portion of the load is disconnected at time $t=0.8s$. The grid current is sinusoidal and amazingly strong, as can be seen in the details. Due to the lower cost of the overall powerful load, the amount of

electricity provided into the system increases. The DC-Link voltage is also stable, remaining close to the regulated value of 700 V.

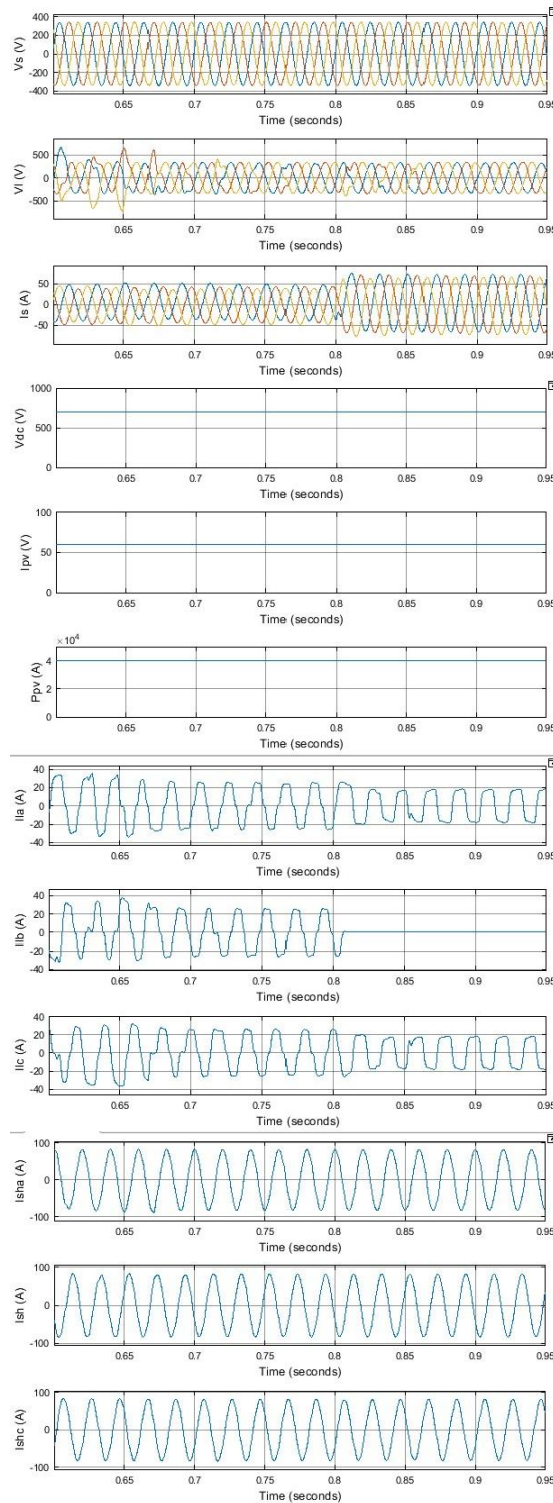
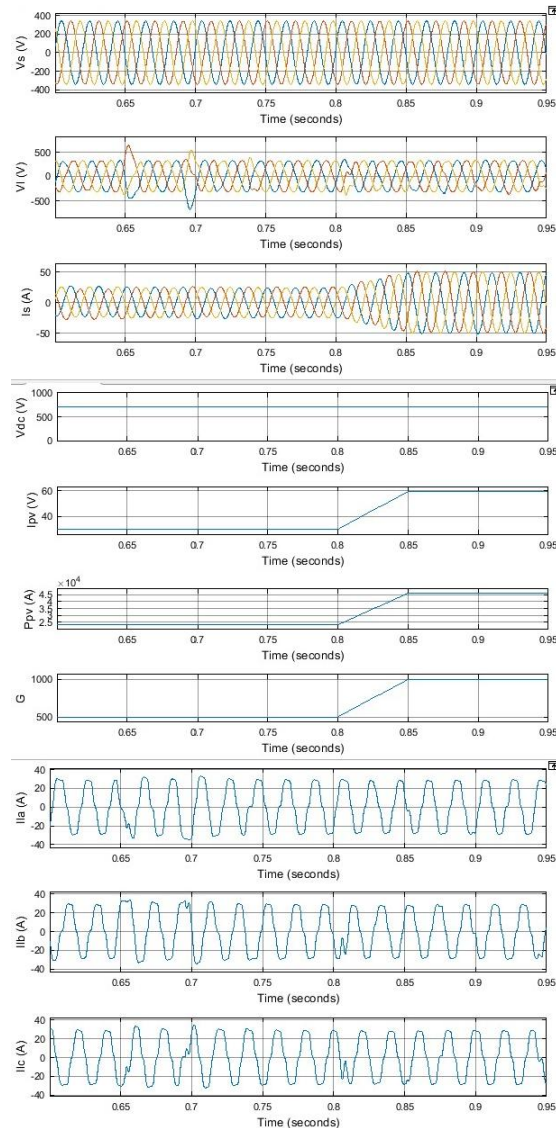


Figure. 16 ANFIS controller PV – UPQC performance under load – unbalance condition.

3. PV-Irradiation UPQC's Irradiation Performance

Under varying solar irradiation, Figure 17 displays the PV-overall UPQC's dynamic performance with the ANFIS controller. Solar irradiation varies between 500W/m^2 at 0.8 seconds and 1000W/m^2 at 0.85 seconds. PV array output will increase as irradiance rises, and grid current day will increase as PV arrays feed power into the grid. Figures 18 and 19 show harmonic spectra and THD load for current day-to-day and grid contemporary using an ANIFS-based controller.



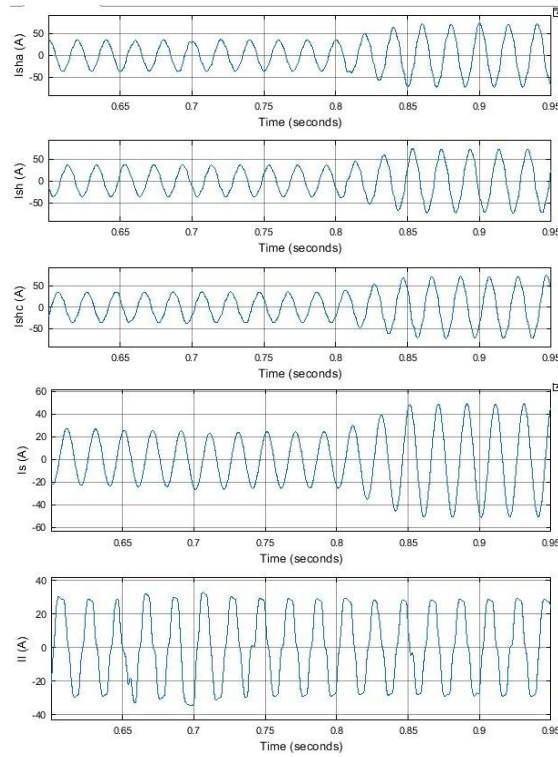
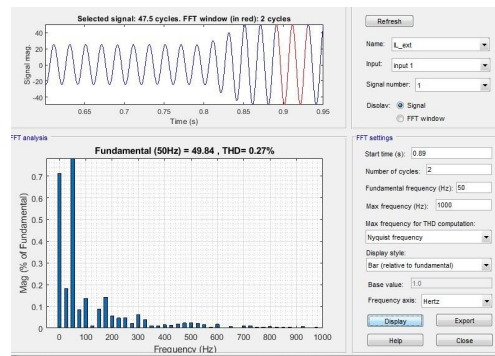
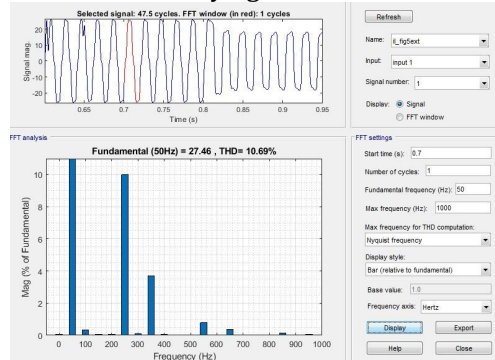


Figure. 17. PV – UPQC Performance under Varying Irradiation Conditions with ANFIS controller



Parameter	% THD	
	With the PI controller [13]	With the ANFIS controller
Current (I_L)	23.46	10.69
Current (I_G)	1.86	0.27

VI.

The dynamic performance of a three-phase PV-UPQC with an ANFIS controller was analyzed under changing irradiance and grid voltage sags/swells in this study. Matlab/Simulink software was used to model the system's performance. PV-UPQC with ANFIS mitigates nonlinear load harmonics and maintains grid current THD with less harmonics than PV-UPQC with PI controller. The system has demonstrated to be stable under varying irradiation, voltage sags/swells, and load unbalance. When a moving average filter was added to d-q management, it improved performance, particularly when the load was unbalanced. PV-UPQC appears to be a promising solution for modern dc micro grids because it combines dispersed generation with power quality enhancement. In comparison to the proposed PI controller, which produces harmonics in load current of 23.46 % and grid current of 1.86 %, the ANIFIS controller-based system produces harmonics in load current of 10.69 % and grid current of 0.27 %.

VII.

- [1] B. Mountain and P. Szuster, "Solar, solar everywhere: Opportunities and challenges for australia's rooftop pv systems," *IEEE Power and Energy Magazine*, vol. 13, no. 4, pp. 53–60, July 2015.
- [2] A. R. Malekpour, A. Pahwa, A. Malekpour, and B. Natarajan, "Hierarchical architecture for integration of rooftop pv in smart distribution systems," *IEEE Transactions on Smart Grid*, vol. PP, no. 99, pp. 1–1, 2017.
- [3] Y. Yang, P. Enjeti, F. Blaabjerg, and H. Wang, "Wide-scale adoption of photovoltaic energy: Grid code modifications are explored in the distribution grid," *IEEE Ind. Appl. Mag.*, vol. 21, no. 5, pp. 21–31, Sept 2015.
- [4] M. J. E. Alam, K. M. Muttaqi, and D. Sutanto, "An approach for online assessment of rooftop solar pv impacts on low-voltage distribution networks," *IEEE Transactions on Sustainable Energy*, vol. 5, no. 2, pp. 663–672, April 2014.
- [5] J. Jayachandran and R. M. Sachithanandam, "Neural network-based control algorithm for DSTATCOM under nonideal source voltage and varying load conditions," *Canadian Journal of Electrical and Computer Engineering*, vol. 38, no. 4, pp. 307–317, Fall 2015.
- [6] A. Parchure, S. J. Tyler, M. A. Peskin, K. Rahimi, R. P. Broadwater, and M. Dilek, "Investigating pv generation induced voltage volatility for customers sharing a distribution service transformer," *IEEE Trans. Ind. Appl.*, vol. 53, no. 1, pp. 71–79, Jan 2017.
- [7] E. Yao, P. Samadi, V. W. S. Wong, and R. Schober, "Residential demand side management under high penetration of rooftop photovoltaic units," *IEEE Transactions on Smart Grid*, vol. 7, no. 3, pp. 1597–1608, May 2016.
- [8] B. Singh, A. Chandra and K. A. Haddad, *Power Quality: Problems and Mitigation Techniques*. London: Wiley, 2015.
- [9] M. Bollen and I. Guo, *Signal Processing of Power Quality Disturbances*. Hoboken: John Wiley, 2006.
- [10] P. Jayaprakash, B. Singh, D. Kothari, A. Chandra, and K. Al-Haddad, "Control of reduced-rating dynamic voltage restorer with a battery energy storage system," *IEEE Trans. Ind. Appl.*, vol. 50, no. 2, pp. 1295–1303, March 2014.
- [11] B. Singh, C. Jain, and S. Goel, "ILST control algorithm of singlestage dual purpose grid connected solar pv system," *IEEE Trans. Power Electron.*, vol. 29, no. 10, pp. 5347–5357, Oct 2014.
- [12] R. K. Agarwal, I. Hussain, and B. Singh, "Three-phase single-stage grid tied solar pv ecs using PLL-less fast CTF control technique," *IET Power Electronics*, vol. 10, no. 2, pp. 178–188, 2017.
- [13] Sachin Devassy; Bhim Singh, "Design and Performance Analysis of ThreePhase Solar PV Integrated UPQC" 2016 IEEE 6th International Conference on Power Systems (ICPS).